41st Aerospace Sciences Meeting and Exhibit
6-9 January 2003, Reno, Nevada

AIAA 2003-496

An experimental study on the energy balance in the repetitively pulsed laser propulsion

Koichi Mori,[1] Hiroshi Katsurayama,[2] Yasuro Hirooka,[2]
Kimiya Komurasaki,[3] and Yoshihiro Arakawa [4]
University of Tokyo, *Bunkyo-ku*, 7-3-1 Hongo, Tokyo, JAPAN

In order to investigate the relation between the impulse and the energy conversion efficiency from laser beam to the blast wave, impulse transferred by a laser-induced blast wave to a conical nozzle was measured using the pendulum method. As a result, the impulse decreased with the increase in the divergence angle of the nozzle, and the momentum-coupling coefficient takes the maximum value with a certain nozzle length. A simplified analysis employing Sedov's blast wave theory has been performed to interpret the experimental results, and a semi-empirical formula, which is based on the analytical expression, was deduced to estimate the impulse. The formula also reproduced another experimental results reported by Ageev et. al.

Introduction

Repetitively Pulse (RP) laser engine consists of a focusing mirror that works also as a diverging nozzle. A laser beam is transmitted remotely from the ground, and it is focused in an atmospheric gas by the mirror. Plasma is produced in the vicinity of the focus, and then it expands quickly to drive a blast wave. During high-speed flight, this engine operates in an air-breathing mode utilizing the atmospheric air introduced through an intake. On the other hand, during low-speed flight, it operates in a pulsejet mode, which has been currently investigated.[1,2]

The energy conversion processes are illustrated schematically in Fig. 1. Laser absorption in a gas is accompanied by propagation of laser-absorption region along the laser light channel.[3] At the laser power density greater than 10^7 W/cm^2, absorption occurs in the Laser Supported Detonation (LSD) regime. At the power density lower than 10^6 W/cm^2, the absorption occurs in the Laser Supported Combustion (LSC) regime.

The absorbed energy is converted into the blast wave energy E_{bw}, radiation loss, and chemical potential energy. Here, the blast wave energy is defined as the sum of translational and kinetic energy within the blast wave. After the blast wave has gone away, a high-temperature region, "fire-ball" remains in the vicinity of the explosion center. The chemical potential of the fire-ball is frozen partly.

Since E_{bw} uniquely determines the pressure distribution within the blast wave, it is useful to characterize the energy conversion from the laser energy E_i to the blast wave energy by the blast wave energy conversion efficiency η_{bw} defined as

$$\eta_{bw} \equiv E_{bw}/E_i \qquad (1).$$

In addition to the energy conversion processes, the conversion from the blast wave energy to the impulse must be understood to predict the performance. The performance of the RP laser engine is described with the momentum coupling coefficient C_m that is defined as the ratio of the impulse I to E_i. Many experimental and theoretical studies have been performed focusing a laser beam on a metal plate surface.[4-8] LSD or LSC wave is formed on the surface, and the plate is pushed both by plasma region produced during the laser heating, and the blast wave. For this flat plate type engine, C_m has been reported to be lower than 0.1 mNs/J.

Higher C_m has been obtained using a diverging nozzle.[2,9,10] Engine cycle of experimental laser pulsejet with a diverging nozzle is illustrated in Fig.2. Focused and intensified laser pulse induces the absorption by air contained in the nozzle volume. Quick expansion of the plasma transfers the absorbed energy into the blast wave energy. After the energy conversion, the blast wave expands pushing the nozzle wall. After the shock wave reaches at the exit of the nozzle, the air exhaustion starts, and the pressure acting on the nozzle wall decreases quickly. Afterward, new air is refilled from the exit plane, and then the pressure recovers to the atmospheric one.

The influence of nozzle size has been investigated for conical nozzles systematically by Ageev et. al.[9] They concluded that there was an optimum nozzle length with a certain input energy. The influence of the input laser energy on C_m has been investigated using parabola (Bell) nozzles.[2,10] These studies also suggest that there would be an optimum input energy for a certain nozzle size.

Each of the specific experimental results, which were performed with a specific set of laser and nozzle, reflect both the energy conversion processes from the laser to the blast wave and the pure characteristics of the nozzle design. However, any quantitative description has not been proposed for the relation between the impulse and the energy conversion processes.

In this experimental study, η_{bw} was measured, and the impulse transferred by the blast wave was measured using conical nozzles in order to purely extract the effect of the nozzle design on C_m.

---

[1] Graduate student, Department of Advanced Energy, Student member AIAA

[2] Graduate student, Department of Aeronautics and Astronautics

[3] Associate professor, Department of Advanced Energy, Member AIAA

[4] Professor, Department of Aeronautics and Astronautics, Member AIAA

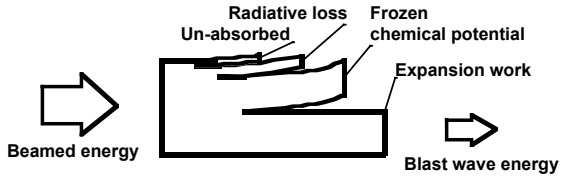

Fig. 1 Energy flow from the beamed energy to the blast wave energy.

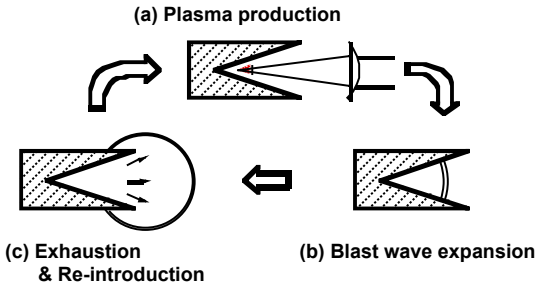

Fig. 2 Conversion processes from laser beam to the impulse.

Blast wave energy conversion efficiency

A TEA CO_2 laser was used and E_i was changed from 2 to 11 J by inserting polyethylene sheets, whose thickness was 20 μm. The duration of the laser pulse was mostly 3 μs. The laser beam was focused using an off-axial parabola mirror.

Blast wave energy has been obtained from the shadowgraph images of the laser-induced shock wave, which are shown in Fig. 3. The experimental apparatus and analysis methods are presented in our previous reports.[11-13] Figure 4 shows the relation between E_i and E_{bw}. The error in E_{bw} was mostly originated from the fluctuation in E_i. E_{bw} was proportional to E_i, and η_{bw} was found 0.47 ± 0.05. The efficiency was insensitive to the input laser energy within the tested range.

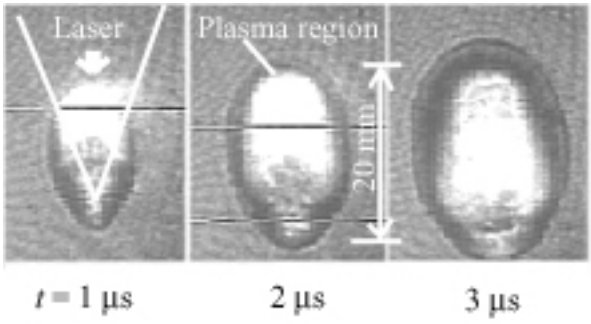

Fig. 3 Shadowgraph: (E_i = 10 J).

Experimental apparatus

The experimental apparatus is illustrated schematically in Fig. 5. The *f*-number of the focusing optics was 3.3. Plasma was produced in the vicinity of the apex of a conical nozzle under an atmospheric air. The temperature and the humidity were controlled by an air-conditioner at 20 ℃ and 50 %, respectively.

A ballistic pendulum was used to measure the impulsive thrust. The pendulum arm was supported by a ball bearing. The pendulum movement was measured using a laser displacement sensor. After an impulse is imparted at the end of the arm, the pendulum oscillates with a cycle of mostly two seconds, as shown in Fig. 6(a). The displacement decayed due to the friction of the bearing. Theoretically, the motion is described by an equation:

$$I\ddot{\theta} + c\dot{\theta} + k\theta = 0 \qquad (2)$$

where θ is the angular displacement of the pendulum, I, the moment of inertia, c, the decay constant, and k is defined as

$$k \equiv I\left\{\omega^2 + \left(\frac{c}{2I}\right)^2\right\} \qquad (3)$$

where ω is the frequency of the oscillation. Solving Eq. (2), the displacement of the pendulum is described as

$$\Delta X(t) = P\frac{l^2}{I\omega}\left\{\exp\left(-\frac{c}{2I}t\right)\sin\omega t\right\} \qquad (4)$$

where P and l are impulse imparted at the end of the pendulum and the length of the pendulum arm, respectively. According to this solution, the impulse is proportional to the maximum amplitude of the displacement.

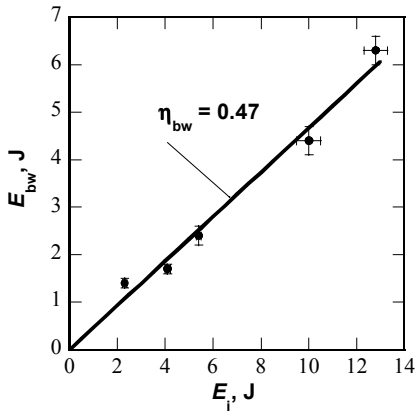

Fig. 4 E_{bw} v.s. E_i.

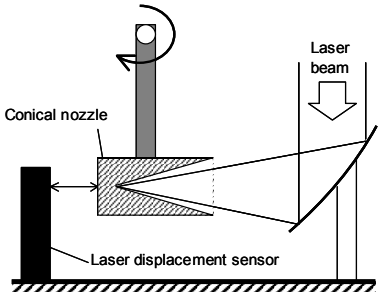

Fig. 5. Experimental apparatus

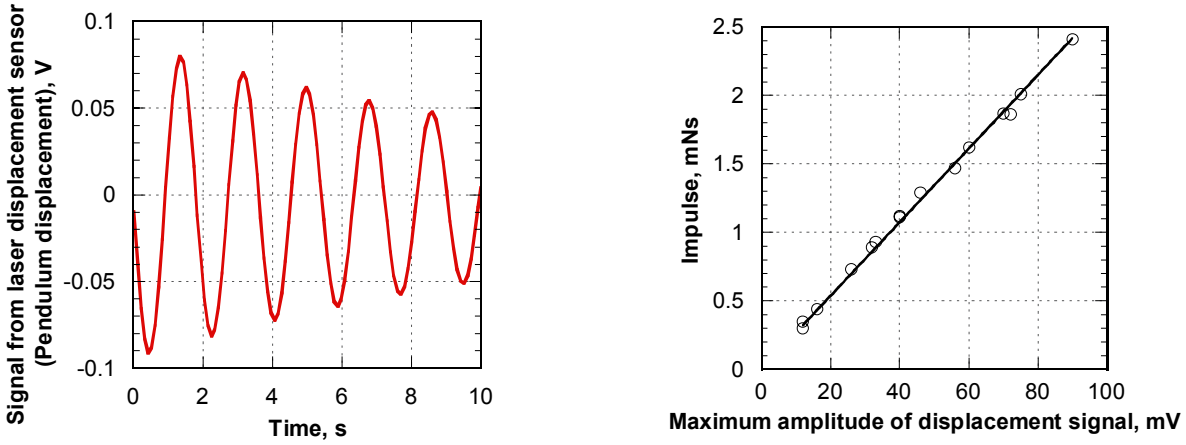

Fig. 6. Measured results: (a) displacement; (b) calibration.

Calibration was performed using a hammer, which hits the exit plane of the nozzle. Imparted impulse was measured using a load cell attached at the head of the hammer. The relation between the impulse and the maximum amplitude of the displacement signal is shown in Fig. 6(b).

In order to investigate the effect of the divergence angle of the nozzle on C_m, the impulse was measured changing the angle while keeping the cross-sectional diameter of the nozzle exit at 25 mm. The impulse was also measured with various nozzle lengths keeping the divergence angle at 15 degrees. The outer shape of the nozzle was fabricated to be cylinder to remove the influence of the outer shape on the impulse. Measurement was conducted five times for each condition.

Experimental results

The relation between the half divergence angle α_d of the conical nozzle and the momentum-coupling coefficient C_m ($\equiv I / E_i$) is shown in Fig. 7. The maximum C_m was recorded with the minimum α_d of 10 degrees, and C_m decreased exponentially with the increase in α_d.

The relation between C_m and the nozzle length is shown in Fig. 8 where a scaling parameter r represents the nozzle length. r is defined as

$$r \equiv \frac{R_n}{R^*} \qquad (5)$$

where R_n is the actual nozzle length, as illustrated in Fig. 9, and R^* is a characteristic radius of shock wave defined as

$$R^* \equiv \left(\frac{E_i / \sin^2(\alpha_d / 2)}{p_a} \right)^{\frac{1}{3}} \qquad (6)$$

where p_a is the ambient pressure. R^* is a measure of the strength of explosion, and this is equivalent to the radius of the shock wave R_s when the pressure at the shock front decayed mostly to the atmospheric one.

In this measurement, five nozzles, which are different in R_n with each other, were tested, and E_i was varied from 6 to 11 J for each nozzle. As a result, the influence of R_n, and E_i on C_m can be expressed adequately using a scaling parameter r. C_m increased with r smaller than 0.3 and began to decrease with r.

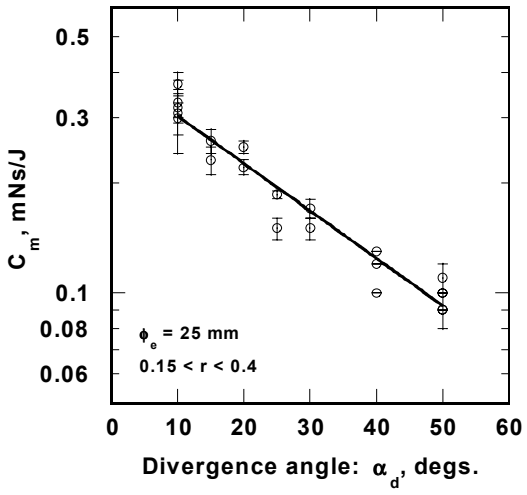

Fig. 7 Influence of α_d on C_m

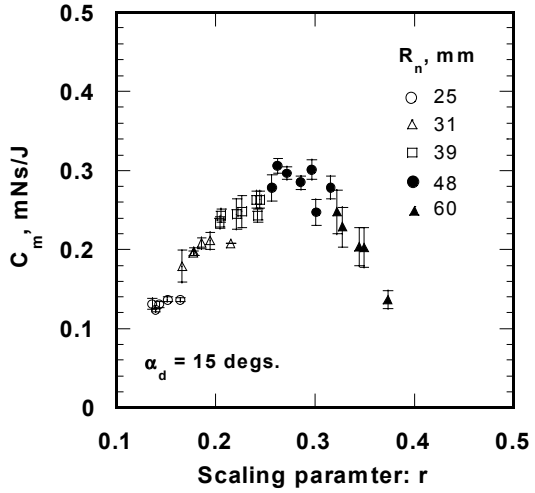

Fig. 8 Influence of the nozzle length on C_m.

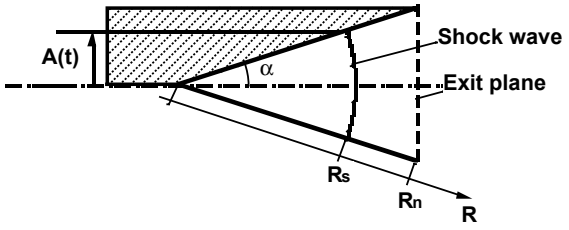

Fig 9 Schematic of the propagation of shock wave in a conical nozzle

Discussions

Blast wave theory

Simplified analysis has been performed to interpret the experimental results. It is assumed that the laser beam is focused into the apex of the cone and that the absorption processes were accomplished instantaneously. Impulse imparted to a conical nozzle I_{net} is described as

$$I_{\text{net}} = \int_o^{t_{arr}} \int_A \left(p(t,A) - p_a \right) dA dt \qquad (7)$$
$$= I^+ - I^-$$

where

$$I^+ \equiv \int_o^{t_{arr}} \int_A p(t,A)\, dA dt \qquad (8).$$
$$I^- \equiv \int_o^{t_{arr}} \int_A p_a dA dt$$

Here, t_{arr} is the time when the shock wave arrives at the exit of the cone, A is the cross sectional area, and $p(t,A)$ is the pressure in the compressed region behind the shock wave. The pressure within the cone is assumed to recover to the atmospheric one instantaneously after the shock wave arrives at the exit.

Kompaneets approximation allows us to consider the pressure to be homogeneous,[14] and $p(t,A)$ is written as $p(t)$. I^+ and I^- can be written again as

$$I^+ = \int_o^{t_{arr}} p(t)\, A(t) dt \qquad (9)$$
$$I^- = \int_o^{t_{arr}} p_a A(t) dt$$

where $A(t)$ is the pressurized area that is perpendicular to the exit plane, as shown in Fig. 9. In addition, time-varying thrust $F(t)$ is written as

$$F(t) = \{ p(t) - p_a \} A(t) \qquad (10)$$

$p(t)$ is a function of the blast wave energy E_{bw} and the blast wave volume $V_{\text{bw}}(t)$:

$$p(t) = (\gamma - 1) \frac{E_T}{V_{bw}(t)} \qquad (11)$$
$$E_T = \beta_T E_{bw}$$

where γ the specific heat ratio, E_{T} is the internal energy within the blast wave, and β_{T} is the ratio of the internal energy to the blast wave energy. According to Sedov solution,[15] β_{T} = 7/9. The time varying radius of shock wave $R_s(t)$ is described in the Sedov solution as

$$R_s(t) = \xi_0 \left(\frac{E_0}{\rho_a} \right)^{\frac{1}{5}} t^{\frac{2}{5}} \qquad (12),$$

where ξ_0 is a function of γ whose value is 1.03 when γ = 1.4, and $E_0 \equiv E_{bw} / \sin^2(\alpha_d/2)$, and r_{a} is the ambient density. Accordingly, $V_{\text{bw}}(t)$ is written as

$$V_{bw}(t) = \frac{4\pi}{3} \sin^2\left(\frac{\alpha_d}{2} \right) \{ R_s(t) \}^3 \qquad (13).$$

From Eqs. (11-13), $p(t)$ and $A(t)$ are formulated as

$$p(t) = \left\{ \frac{3(\gamma-1)\beta_T}{4\pi \xi_0^{\,3}} \rho_a \left(\frac{E_0}{\rho_a} \right)^{2/5} \right\} t^{-6/5} \qquad (14),$$

and

$$A(t) = \left\{ \pi \xi_0^{\,2} \left(\frac{E_0}{\rho_a} \right)^{2/5} \sin^2 \alpha_d \right\} t^{4/5} \qquad (15).$$

From Eqs. (9), (14), and (15), formula for I^+ and I^- are obtained as

$$I^+ = \frac{1}{C_a} \sqrt{\frac{\gamma}{\xi_0^{\,5}}} f(\alpha_d) \left\{ \frac{5(\gamma-1)\beta_T}{4} \sqrt{\eta_{bw}} E_i \right\} r^{\frac{3}{2}} \qquad (16),$$
$$I^- = \frac{1}{C_a} \sqrt{\frac{\gamma}{\xi_0^{\,5}}} f(\alpha_d) \left\{ \frac{5\pi}{9} \frac{1}{\sqrt{\eta_{bw}}} E_i \right\} r^{\frac{9}{2}}$$

where

$$f(\alpha_d) = \left(\frac{\sin \alpha_d}{\sin \alpha_d / 2} \right)^2 \qquad (17),$$

and from Eq. (7),

$$C_m = \frac{1}{C_a} \sqrt{\frac{\gamma}{\xi_0^{\,5}}} f(\alpha_d) \left[\left\{ \frac{5(\gamma-1)\beta_T}{4} \sqrt{\eta_{bw}} \right\} r^{\frac{3}{2}} - \left\{ \frac{5\pi}{9} \frac{1}{\sqrt{\eta_{bw}}} \right\} r^{\frac{9}{2}} \right] \qquad (18).$$

The Sedov solution assumes that the shock is so strong that $p(t)$ is much larger than p_{a}.[16] Since this assumption on the pressure is equivalent to the condition that I^+ is much larger than I^-, this model is valid as long as r is smaller than the critical value that gives the maximum C_{m}.

In Fig. 10(a), the theoretical values are compared with the experimental results on the influence of α_{d}, which is shown in Fig. 7. For the theoretical curve, η_{bw} has been set at the measured value; 0.47. The theory overestimates C_{m}, and it decreases with α_{d} less sharply than the measured plots.

In Fig. 10(b), theoretical C_{m} is compared with the experimental results for the influence of the nozzle length. Although theory overestimates C_{m}, theoretical C_{m} takes the maximum value at $r \sim 0.3$, and this tendency agrees with the experimental results.

As these results suggest, although the theory can regenerate the relation between r and C_{m} qualitatively, the effect of α_{d} cannot be regenerated sufficiently, and $f(\alpha_{\text{d}})$ of Eq. (17) is suspected inadequate. The discrepancy between the theoretical curve and the measured plots should be due to the assumption that the thrust during the exhaustion and refilling processes (See (c) in Fig. 2) is ignored in this theory.

Semi-empirical formula

From Eq. (18), $f(\alpha_{\text{d}})$ can be written as a function of C_{m} as

$$f(\alpha_d) = C_m C_a \sqrt{\frac{\xi_0^{\,5}}{\gamma}} \left[\left\{ \frac{5(\gamma-1)\beta_T}{4} \sqrt{\eta_{bw}} \right\} r^{\frac{3}{2}} - \left\{ \frac{5\pi}{9} \frac{1}{\sqrt{\eta_{bw}}} \right\} r^{\frac{9}{2}} \right]^{-1} \qquad (19).$$

Empirically deduced values of $f(\alpha_{\text{d}})$ were calculated substituting the empirical C_{m} plotted in Fig. 10(a) into Eq. (19). The empirical value of $f(\alpha_{\text{d}})$; $f_{\text{e}}(\alpha_{\text{d}})$ is plotted in Fig. 11. Since $f_{\text{e}}(\alpha_{\text{d}})$ decreased with α_{d} exponentially, $f_{\text{e}}(\alpha_{\text{d}})$ can be expressed as

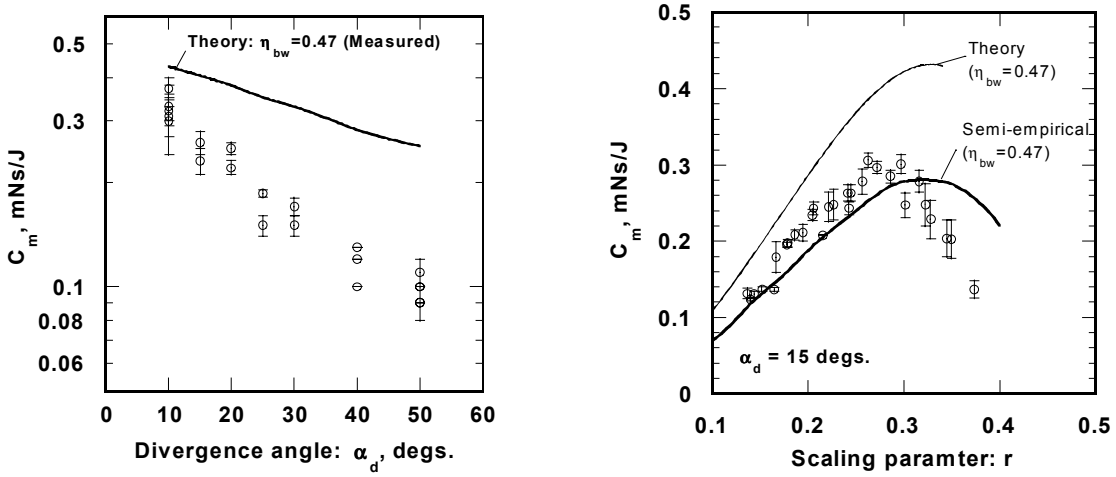

Fig. 10 Comparison between the measured and theoretical results: (a) angular dependency; (b) scaling relation.

$$f_e(\alpha_d) = A_0 \exp\left[-\frac{\alpha_d}{\alpha_0}\right] \quad (20).$$

where A_0 and α_0 are deduced fitting an exponential function to the $f_e(\alpha_d)$ plots through the least square method. As a consequence, A_0 was found 3.54, and α_0, 47.2 degrees.

Semi-empirical formula for C_m is obtained replacing the theoretical $f(\alpha_d)$ to the empirical $f_e(\alpha_d)$. The r-C_m relation calculated using the semi-empirical formula is compared with the experimental results in Fig. 10(b). Reasonable agreement between the formula and the experimental was confirmed at $r <$ 0.3.

Thrust history

From Eq. (10), Semi-empirical expression for the time-varying thrust can be written as

$$F(t) = \left\{\frac{3(\gamma-1)\beta_T}{4\xi_0}\rho_a\left(\frac{E_0}{\rho_a}\right)^{4/5} t^{-2/5} - \pi\xi_0^2\left(\frac{E_0}{\rho_a}\right)^{2/5} t^{4/5}\right\} \times \sin^2\left(\frac{\alpha_d}{2}\right) A_0 \exp\left(-\frac{\alpha_d}{\alpha_0}\right) \quad (21).$$

In Fig. 12, temporal change in the thrust is drawn. The duration of the positive thrust is extended as R_n increases from 30 to 60 mm, and then the impulse increases with R_n and also with r. However, as R_n increases further from 60 to 90 mm, $p(t)$ becomes lower than p_a, and the thrust turns to be negative at later times. As a consequence, the impulse decreases with R_n larger than a certain critical value. The flow condition in the nozzle can be called "Under expansion" when the nozzle is shorter than the critical value, and "Over expansion" when it is longer than the critical value. Accordingly to the merge of two expansion conditions, C_m takes the maximum value at the specific r where $p(t_{arr}) = p_a$.

Comparison with Ageev's experimental results

The curve deduced from the formula is compared with Ageev's experimental results[7] in Fig. 13. Reasonable agreement between the curve by the formula and experimental values is confirmed both for the effect of a_d and r when η_{bw} is 0.8.

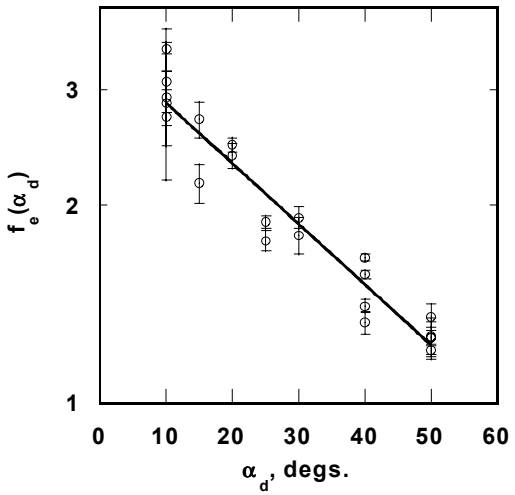

Fig. 11. Experimentally deduced $f_e(\alpha_d)$.

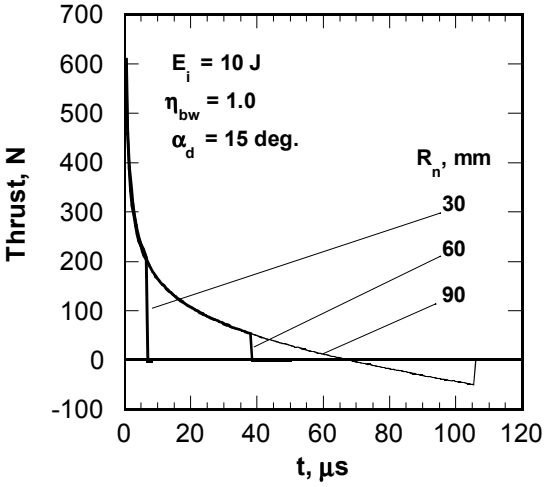

Fig. 12. Time varying thrust deduced using the empirical formula.

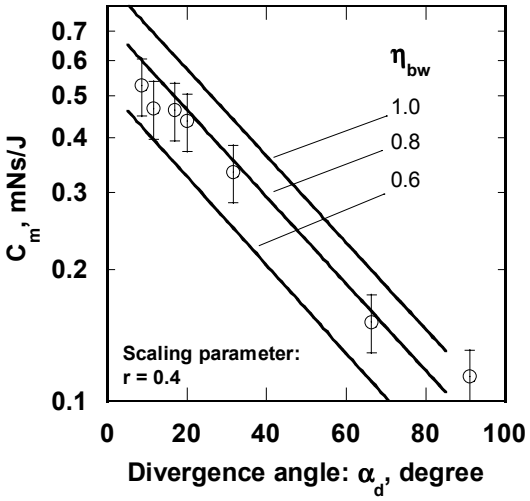

(a)

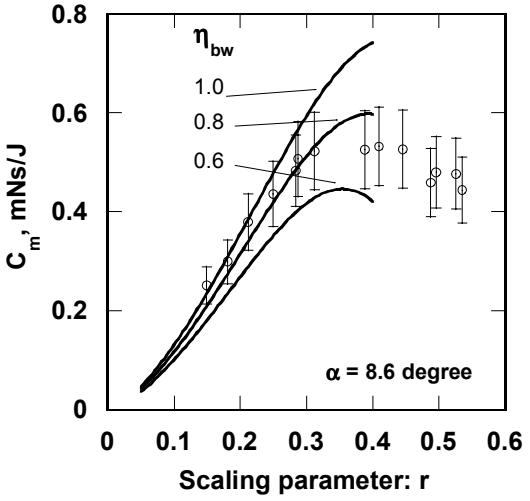

(b)

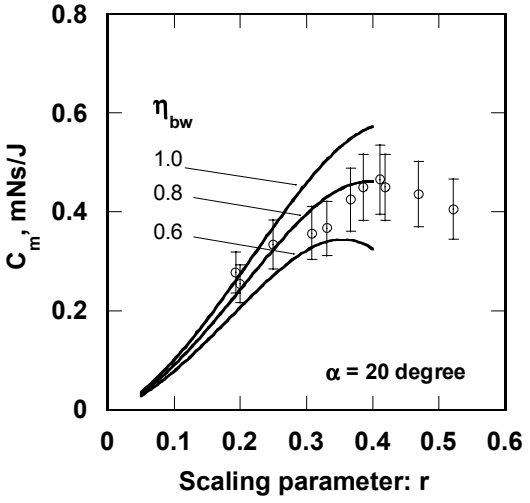

(c)

Fig.13 Comparison between the Semi empirical and Ageev's experimental results: (a) Effect of α_d; (b) effect of *r* α_d = 8.6 degs.; (c) α_d = 20 degs.

Conclusion

Impulse imparted by a laser-induced blast wave on a conical nozzle has been measured using the pendulum method. As a result, the momentum-coupling coefficient decreased with the divergence angle of the nozzle, and it became maximum at a certain nozzle length that satisfies the condition; $r = 0.4$. Semi empirical formula has been proposed to estimate the relation between the momentum-coupling coefficient and the blast wave energy conversion efficiency. Deduced formula regenerated Ageev's experimental results when the efficiency was set at 0.8.

References

[1] Myrabo, L. M., Messitt, D. G., and Mead, Jr., F. B., AIAA Pap. 98–1001, 1998.

[2] Schall, W. O., *Proceedings of High-Power Laser Ablation III, Santa Fe, NM*, 2000, SPIE, Bellingham, WA, 2000, p. 472.

[3] Raizer, Y. P.: *Laser-Induced Discharge Phenomen*a, Studies in Soviet Science Consultants Bureau, New York, 1977, p.199.

[4] Pirri, A. N., Schlier, and Northam, D., Appl. Phys. Lett., **21**, 79 (1972).

[5] Pirri, A. N., Phys. Fluids, **16**, 1435 (1973).

[6] Ferriter, N., Maiden, D. E., Winslow, A. M., and Fleck Jr., J. A., AIAA J., **15**, 1597 (1977).

[7] Reilly, J. P., Ballantyne, A., and Woodroffe, J. A., AIAA J., **17** 1098 (1978).

[8] Simons, G. A., AIAA J., **22**, 1257 (1984).

[9] Ageev, V. P., Barchukov, A. I., Bunkin, F. V., Konov, V. I., Korobeinikov, V. P., Putjatin, B. V., and Hudjakov, V. M., Acta Astronautica **7**, 79 (1980) .

[10] Myrabo, L. M., Messitt, D. G., and Mead, Jr., F. B., AIAA Pap. 2002–3783, 2002.

[11] Mori, K., Komurasaki, K., Katsurayama, H., and Arakawa, Y., AIAA Pap. 2001-0649.

[12] Mori, K., Komurasaki, and Arakawa, Y., AIAA Pap. 2002-0634.

[13] Mori, K. Komurasaki, K., and Arakawa, Y., J. Appl. Phys, **92**, 10 (2002).

[14] Kompaneets, A. S., Soviet Phys. Dokl. **5**, 46 (1960).

[15] Sedov, L. I.: Similarity and Dimension Methods in Mechanics (Academic Press, New York, 1959).

[16] Zel'dovich, Y. B., and Raizer, Y. P.: *Physics of Shock waves and High-temperature Hydrodynamics Phenomena*, Academic Press, New York, 1967.